Stress Distribution Analysis of Bell Crank Lever Using Theoretical, Photoelasticity, and Computational Methods

Mrs.D.Divya Chandrika[1], Mrs.A.Jyothi[2], Mr.R.Sagar, [3] Mr.B.Venkata Rao[4]
[1,2,3,4] *Assistant professor, Department of Mechanical Engineering, Wellfare Institute of Science, Technology and Management-Pinagadi-Pendurthi-Visakhapatnam-Andhrapradesh-531173*

***Abstract*—A Bell Crank Lever is a bar that rotates about a fixed point, commonly used in railway signaling, Hartnell-type governors, and air pump drives in condensers. It functions to lift loads with minimal effort while altering motion through angles, typically 90° or 180°. The primary stresses in the lever are bending stress at the fulcrum and shear stress on the fulcrum pin, with maximum stress concentration at the fulcrum. This study focuses on the stress analysis of the Bell Crank Lever within an angle range of 90° to 180°, employing the Finite Element Method (FEM) using ANSYS Workbench 14.5 and photoelasticity as an experimental validation technique. The experimental analysis utilizes photoelastic sheets of Araldite with hardener HY-951 and curing agent CY-230. A comparison of analytical and experimental results demonstrates close agreement, confirming the accuracy of the stress analysis.**

***Index Terms*—Bell Crank Lever, Stress Analysis, Finite Element Method, ANSYS, Photoelasticity.**

I. INTRODUCTION:

Stress analysis is a fundamental aspect of engineering that involves evaluating the internal stresses and deformations within materials and structures subjected to various forces or loads. It is crucial in ensuring structural integrity, safety, and optimal performance across multiple engineering domains, including civil, mechanical, and aerospace engineering. The analysis plays a key role in the design, optimization, and maintenance of structures ranging from bridges, tunnels, and dams to aircraft, rockets, mechanical components, and even small-scale items like plastic cutlery and staples. Stress analysis is essential not only during the design phase but also for maintenance and failure investigation.

The current study focuses on the stress analysis of a Bell Crank Lever, a mechanical component used in applications like railway signaling, Hartnell-type governors, and air pump drives. The Bell Crank Lever functions by converting applied forces into motion at different angles, typically 90° or 180°. Since it experiences bending stress at the fulcrum and shear stress at the fulcrum pin, analyzing the stress distribution is essential to ensure its strength and durability under operational conditions. By comparing the theoretical results, analytical results from ANSYS simulations with the experimental results from photoelastic analysis, the study verifies the accuracy of the

stress distribution predictions. The close agreement between the two methods confirms the reliability of the analysis, making it a valuable approach for designing and optimizing Bell Crank Levers in practical applications.

II. EXPERIMENTAL STRESS ANALYSIS:

The Bell Crank Lever is designed to lift a load with minimal applied effort. For its analysis, the most critical area is identified, and based on this, a two-dimensional model of the lever is developed. Various shapes of the Bell Crank Lever are illustrated in the figures below. To evaluate its performance, three different loads—100N, 150N, and 200N—are applied at one end**,** and the resulting stresses are determined.

It is the force which is to be applied to the machine to lift the load or to overcome the resistance. It is denoted by P and has the unit of force.

Length of lever arm in mm (FB) = 50 mm;

Load applied on the lever (W) = 100 N;

Length of effort arm in mm (FA) = 55 mm;

a) Effort(P) when load(W) is 100N, angle between lever arm and effort arm is 90^0

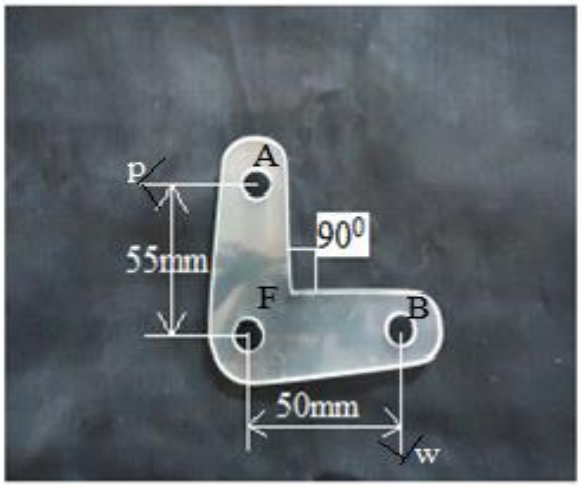

Figure .1 Bell Crank Lever with 90^0

Calculation of the effort (P) required to raise the load (W) 100 N.

Taking moments about the fulcrum (F)

$W \times 50 = P \times 55$

$100 \times 50 = P \times 55$

$\therefore P = 90.90$ N

Resultant force at the fulcrum at F,

$R_F^2 = (W^2 + P^2)$

$R_F^2 = (100^2 + 90.90^2)$

$R_F = 135.14$ N;

Resultant force at the fulcrum (R_F) =135.14N;

b) Effort(P) when load(W) is 150N, angle between lever arm and effort arm is 90^0

Taking moments about the fulcrum (F)

$W \times 50 = P \times 55$

$150 \times 50 = P \times 55$

$\therefore P = 136.36$N

Resultant force at the fulcrum at F,

$R_F^2 = (W^2 + P^2)$

$R_F^2 = (150^2 + 136.36^2)$

$R_F = 202.72$ N;

Resultant force at the fulcrum (R_F) =202.72N;

c) Effort(P) when load(W) is 200N, angle between lever arm and effort arm is 90^0

Taking moments about the fulcrum (F)

$W \times 50 = P \times 55$

$200 \times 50 = P \times 55$

$\therefore P = 181.81$ N;

Resultant force at the fulcrum at F,

$R_F^2 = (W^2 + P^2)$

$R_F^2 = (200^2 + 181.81^2)$

$R_F = 270.30$ N;

Resultant force at the fulcrum (R_F) =270.30N;

Similarly for 120^0, 135^0 and 160^0.

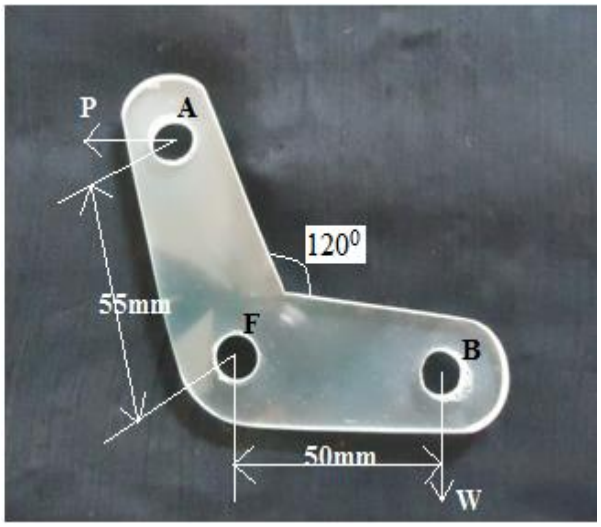

Figure 2. Bell Crank Lever with 120^0

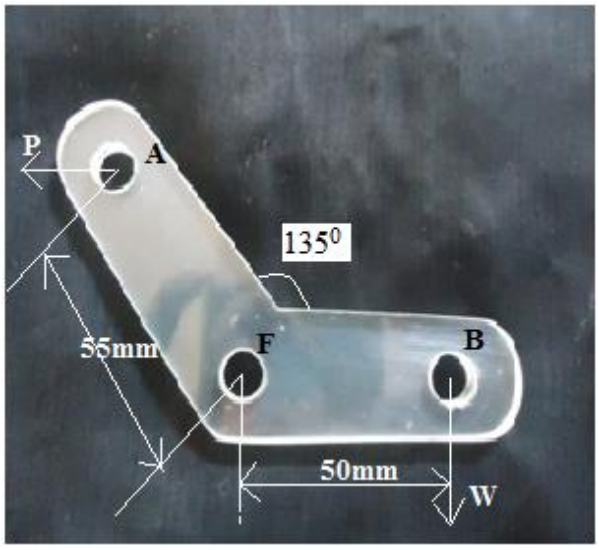

Figure 3. Bell Crank Lever with 135^0

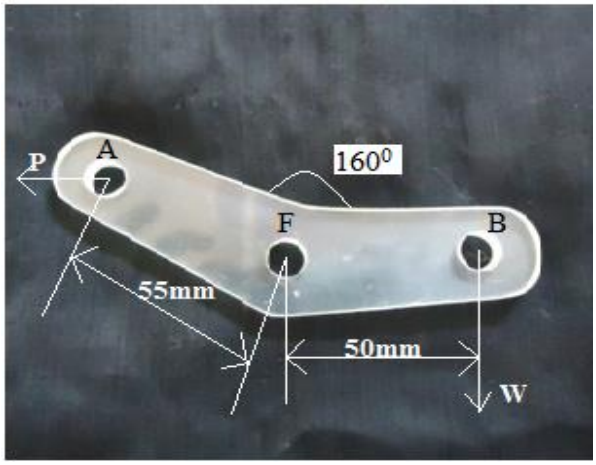

Figure 4. Bell Crank Lever with 160^0

Table 1 Calculation of Effort (P) and Resultant Force (R_F)

Angle	Load in N	Effort in N	Resultant Force (R_F) in N
90^0	100	90.90	135.14
	150	136.36	202.72
	200	181.81	270.30
120^0	100	104.9	177.46
	150	157.45	266.30
	200	209.94	355.05
135^0	100	128.55	211.43
	150	192.84	317.16
	200	257.12	422.90
160^0	100	265.8	361.40
	150	398.7	542.08
	200	531.6	722.80

From the table 1 it is observed that, as the load increases at different angles of Bell Crank Lever, the Effort and also Resultant Force increases. The minimum effort can be applied for a load is observed at an angle of Bell Crank Lever is 90^0. Basing on these values, graph was plotted which is shown in fig.5 between an applied load and the effort.

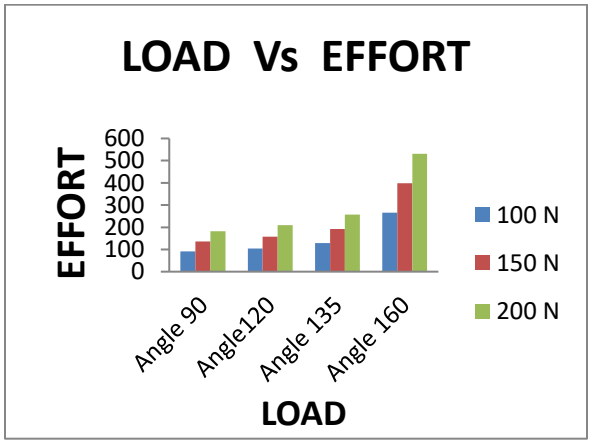

Figure5. Effect of angle between two arms on effort

II.i. Mechanical Advantage:

Mechanical Advantage is defined as the ratio of the load lifted to effort applied. Effort is nothing but the force which is to be applied to the machine to lift the load or to overcome the resistance. It is denoted by P and has the units of force.

Mechanical Advantage (M.A) = Load / Effort

a) The Mechanical Advantage of Bell Crank Lever at $90^{0\ angles}$ as shown in figure 4.1

The load at 100 N,

the Mechanical Advantage = 100/90.90

M.A = 1.10;

The load at 150 N,

the Mechanical Advantage = 150/136.36

M.A = 1.10;

The load at 200 N,

the Mechanical Advantage = 200/181.81

M.A = 1.10;

Similarly for 120^0, 135^0 and 160^0 Mechanical advantage was measured.

From the above calculations it is observed that, as the angle between the lever arms increases, the Mechanical Advantage decreases. The calculated values are as shown in the following table 2.

Table 2 Mechanical Advantage at different angles

Angle	Load(N)	Effort(N)	Mechanical Advantage (M.A)
90^0	100	90.90	1.10
	150	136.36	1.10
	200	181.81	1.10
120^0	100	104.9	0.953
	150	157.45	0.952
	200	209.94	0.952
135^0	100	128.55	0.78
	150	192.84	0.78
	200	257.12	0.78
160^0	100	265.8	0.37
	150	398.7	0.37
	200	531.6	0.37

II.ii Stresses at Lever Section:

Now let us consider Bell Crank Lever at an angle 90^0 as shown in Figure 1 to determine the stresses induced.

Let d= outer boss diameter = 25mm

L = length of lever = 50mm

h= height of the lever arm = 25mm

t = thickness of lever = 5mm

a) W = load = 100N

The maximum bending stress occurs in the lever section:

Bending moment (M) = $W \times L^1 = W (L - d/2)$

M = 3750 N-mm

Section modulus (Z) = $bh^2/6$

$Z = 520.83\ mm^3$

Bending stress (σ_b) = M/Z

$\sigma_b = 7.20\ N/mm^2$

Direct shear stress on the lever (τ):

$\tau = W/(t \times h)$

$\tau = 0.8\ N/mm^2$

Maximum principal stress in the lever section:

$\sigma_{max} = (\sigma_b/2) + (1/2) \times ((\sigma_b)^2 + 4(\tau)^2)^{1/2}$

$\sigma_{max} = 7.28\ N/mm^2$

Maximum shear stress in the lever section:

$\tau_{max} = (1/2) \times ((\sigma_b)^2 + 4(\tau)^2)^{1/2}$

$\tau_{max} = 3.68\ N/mm^2$

Similarly, for 150N and 200N were calculated. From the above calculations the induced stress values are tabulated as below and it is observed that stresses are increased with the applied load.

Table 3 Stresses at the Lever Section

Angle	Load in (N)	Theoretical stresses at lever section (Mpa)	
		σ_{max}	τ_{max}
90^0	100	7.28	3.68
	150	10.93	5.53
	200	14.57	7.37

II.iii. Stresses at Fulcrum pin:

a) The stresses at the Fulcrum pin of Bell Crank Lever of angle 90^0 as shown in figure 1, when the load is 100N and resultant force is 135.14 N

Length of the pin=35mm;

Diameter of the pin=10.18mm;

The pin is in double shear and τ is the shear stress developed in the pin, then

$R = (\Pi/4) \times d^2 \times 2\tau$

Therefore

$\tau = 2R / \Pi d^2 = 2 \times 135.14 / (\Pi \times 10.18^2)$

$\tau = 0.83\ N/mm^2$

Bending moment occurs at the centre of the pin:

$\sigma_b = M / Z$

Where $M = (R/2) \times (l/4 + t/3)$

Where $t = 5mm$

Therefore $M = 703.85$ N-mm

$Z = (\Pi/32) \times d^3$

$Z = 103.57\ mm^3$

$\sigma_b = 6.79\ N/mm^2$

Maximum principal stress developed in pin:

$\sigma_{max} = (\sigma_b/2) + (1/2) \times (\sigma_b^2 + 4\tau^2)^{1/2}$

$\sigma_{max} = 6.89\ N/mm^2$

Maximum shear stress developed in pin:

$\tau_{max} = (1/2) \times (\sigma_b^2 + 4\tau^2)^{1/2}$

$\tau_{max} = 3.49\ N/mm^2$.

Similarly, for 150N and 200N were calculated.

b) The stresses at the Fulcrum pin of Bell Crank Lever of angle 120^0 as shown in figure 2, when the load is 100N and resultant force is 177.46 N

Length of the pin=35mm;

Diameter of the pin=10.18mm;

The pin is in double shear and τ is the shear stress developed in the pin, then

$R_F = (\Pi/4) \times d^2 \times 2\tau$

Therefore

$\tau = 2 R_F / \Pi d^2 = 2 \times 177.46 / (\Pi \times 10.18^2)$

$\tau = 1.09\ N/mm^2$

Bending moment occurs at the centre of the pin:

$\sigma_b = M / Z$

Where $M = (R/2) \times (l/4 + t/3)$

Where $t = 5mm$

Therefore $M = 924.21$ N-mm

$Z = (\Pi/32) \times d^3$

$Z = 103.57\ mm^3$

$\sigma_b = 8.92\ N/mm^2$

Maximum principal stress developed in pin:

$\sigma_{max} = (\sigma_b/2) + (1/2) \times (\sigma_b^2 + 4\tau^2)^{1/2}$

$\sigma_{max} = 9.05\ N/mm^2$

Maximum shear stress developed in pin:

$\tau_{max} = (1/2) \times (\sigma_b^2 + 4\tau^2)^{1/2}$

$\tau_{max} = 4.59\ N/mm^2$.

Similarly, for 150N and 200N were calculated.

c) The stresses at the Fulcrum pin of Bell Crank Lever of angle 135^0 as shown in figure 3, when the load is 100N and resultant force is 211.43 N

Length of the pin=35mm;

Diameter of the pin=10.18mm;

The pin is in double shear and τ is the shear stress developed in the pin, then

$R_F = (\Pi/4) \times d^2 \times 2\tau$

Therefore

$\tau = 2 R_F / \Pi d^2 = 2 \times 211.43 / (\Pi \times 10.18^2)$

$\tau = 1.29\ N/mm^2$

Bending moment occurs at the centre of the pin:

$\sigma_b = M / Z$

Were

$M = (R/2) \times (l/4 + t/3)$

Where t = 5mm

Therefore

M = 1101.13 N-mm

$Z = (\Pi/32) \times d^3$

$Z = 103.57\ mm^3$

$\sigma_b = 10.63\ N/mm^2$

Maximum principal stress developed in pin:

$\sigma_{max} = (\sigma_b/2) + (1/2) \times (\sigma_b^2 + 4\tau^2)^{1/2}$

$\sigma_{max} = 10.78\ N/mm^2$

Maximum shear stress developed in pin:

$\tau_{max} = (1/2) \times (\sigma_b^2 + 4\tau^2)^{1/2}$

$\tau_{max} = 5.47\ N/mm^2$.

Similarly, for 150N and 200N were measured.

d) The stresses at the Fulcrum pin of Bell Crank Lever of angle 160^0 as shown in figure 4, when the load is 100N and resultant force is 361.4N

Length of the pin=35mm;

Diameter of the pin=10.18mm;

The pin is in double shear and τ is the shear stress developed in the pin, then

$R_F = (\Pi/4) \times d^2 \times 2\tau$

Therefore $\tau = 2\ R_F / \Pi\ d^2$

$=2\times361.4 / (\Pi \times 10.18^2)$

$\tau = 2.22\ N/mm^2$

Bending moment occurs at the centre of the pin:

$\sigma_b = M / Z$

Where $M = (R/2) \times (l/4 + t/3)$

Where t = 5mm

Therefore M = 1882.17 N-mm

$Z = (\Pi/32) \times d^3$

$Z = 103.57\ mm^3$

$\sigma_b = 18.17\ N/mm^2$

Maximum principal stress developed in pin:

$\sigma_{max} = (\sigma_b/2) + (1/2) \times (\sigma_b^2 + 4\tau^2)^{1/2}$

$\sigma_{max} = 18.43\ N/mm^2$

Maximum shear stress developed in pin:

$\tau_{max} = (1/2) \times (\sigma_b^2 + 4\tau^2)^{1/2}$

$\tau_{max} = 9.35\ N/mm^2$.

Similarly, for 150N and 200N were measured.

From the above calculations the values are listed in the table 4, and it is observed that, as the load and angle between the arms increases, the maximum principal and shear stresses also increases. The results obtained theoretically at different conditions are graphically shown in fig. 4.6.

Table 4 Stresses at the Fulcrum Pin

Angle	Load in N	Resultant force(R_F) in N	Theoretical stress at fulcrum pin (Mpa)	
			σ_{max}	τ_{max}
90^0	100	135.14	6.89	3.49
	150	202.72	10.34	5.24
	200	270.30	13.79	6.99
120^0	100	177.46	9.05	4.59
	150	266.30	13.58	6.89
	200	355.05	18.11	9.18
135^0	100	211.43	10.78	5.47
	150	317.16	16.18	8.21
	200	422.90	21.57	10.94
160^0	100	361.40	18.43	9.35
	150	542.08	27.66	14.03
	200	722.80	36.87	18.70

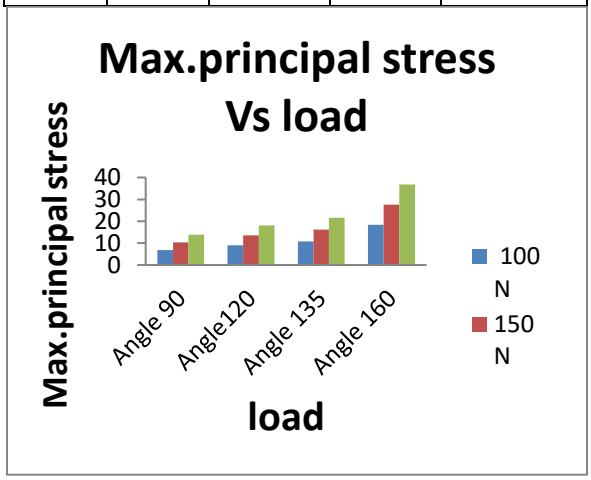

Figure5. Effect of angle between two arms on max.principal stress (Theoretical)

III. EXPERIMENTAL STRESS ANALYSIS:

Experimental stress analysis was done by photoelastic method. In photoelastic method, circular polariscope is used. For determining the fringe order, a circular disc of same material is used. Photoelastic model of bell crank lever is prepared from 5mm thick sheet casted from epoxy resin (mixture of Araldite CY 230 and hardener HY 951). Also, circular shaped disc (calibration disc) of 65mm diameter is prepared from the same sheet. This disc is taken and subjected to compressive load in the circular polariscope set up

as shown in figure 6. Calibration was done on the disc to find material fringe value (F_σ).

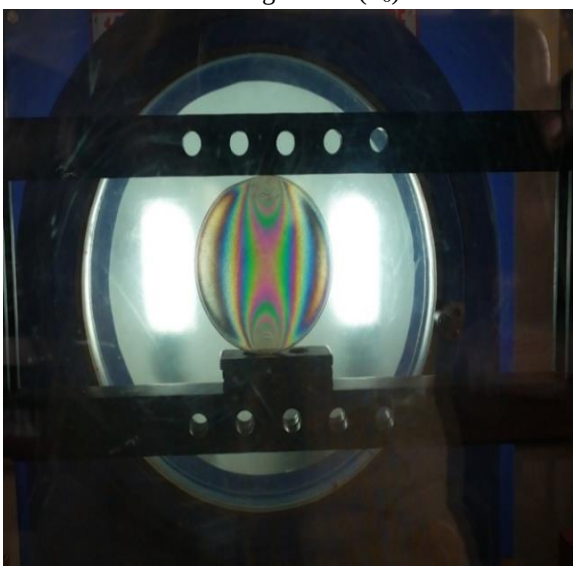

Figure 4.7 Fringe pattern of Calibration disc in white light source

Values of fringe order are noted at different loads as shown in the table 5. Using the formula $F_\sigma = 8P/\pi DN$, material fringe values are determined and average is taken as 12.93 N/mm. where P = Load, N = Fringe order and D = diameter of the disc=65 mm. The material fringe value (F_σ) is the number of fringes produced per unit load. It is the property of the model material for a given wave length and thickness of the model.

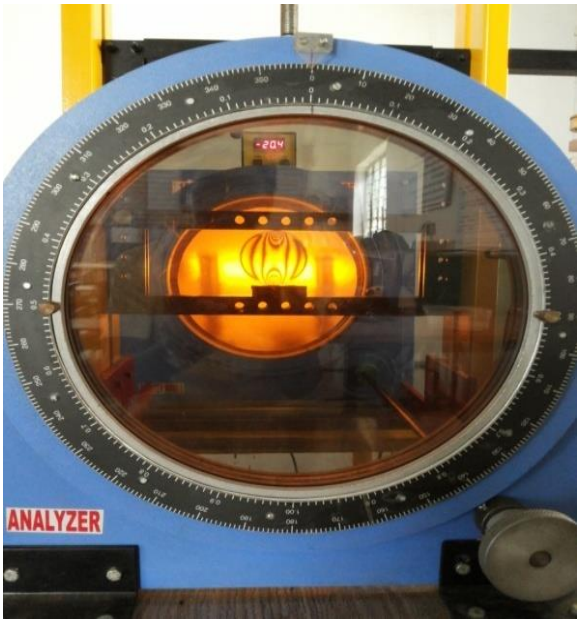

Figure 6 Fringe pattern of Calibration disc in monochromatic light source

Table 5 Determination of Material Fringe Value

S.No.	Load In (N)	Load in (kg)	Fringe Order (N)			Fringe Value (F_σ)	
			Lower (N_l)	Higher (N_h)	(N_l + N_h) /2	F_σ	Avg. (F_σ)
1	100	47.13	1.531	1.669	1.6	11.54	12.93 N/mm
2	150	82.33	2.353	2.461	2.407	13.43	
3	200	91.81	3.242	3.242	2.6	13.83	

III.i Bell Crank Lever of 90^0:

The bell crank lever of 90^0 is kept in circular polariscope arrangement for determining the stresses. At different loads the stresses are found which are listed below.

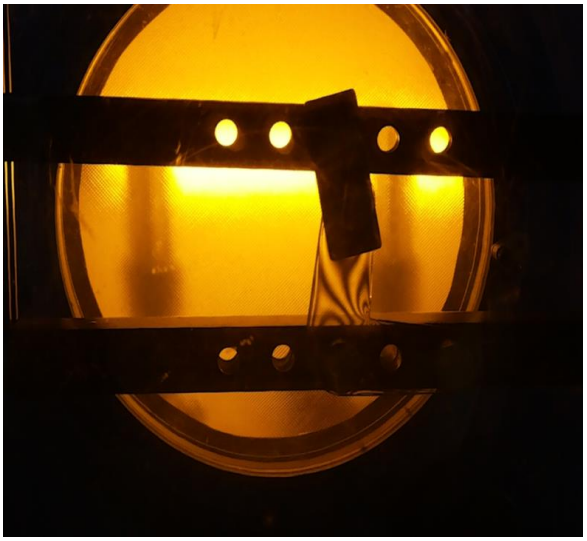

Figure7. Fringes developed in Bell crank lever of 90^0

Table 6. Determination of Stresses using photoelasticity of Bell crank Lever at 90^0

S.No.	Load(kg)	Fringe Order, N	$\sigma = NF\sigma/h$ (MPa)
1	10.2	3.09	8.01
2	15.3	4.65	12.03
3	20.4	6.38	16.52

From the above table 6, it is observed that, as the load increases, the principal stresses also increase.

III.ii. Bell Crank Lever at 120^0:

The bell crank lever at 120^0 is kept in circular polariscope arrangement for determining the stresses. At different loads the stresses are found which are noted below.

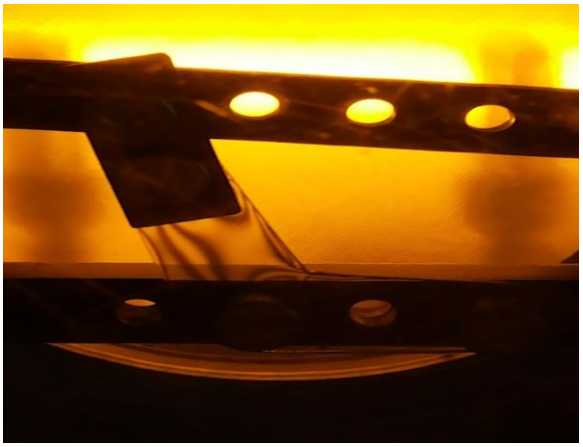

Figure 8. Bell crank lever at 120^0 in Circular polariscope

Table7. Determination of Stresses using photoelasticity of Bell crank Lever at 120^0

S.NO	Load(kg)	Fringe Order, N	σ = NFσ/h (MPa)
1	10.2	4.47	11.58
2	15.3	6.85	17.72
3	20.4	8.96	23.19

From the table 7, it is observed that, as the load increases, the principal stress also increases.

III.iii. Bell Crank Lever at 135^0:

The bell crank lever at 135^0 is placed in circular polariscope arrangement for determining the stresses. At different loads the stresses are found which are noted in below table.

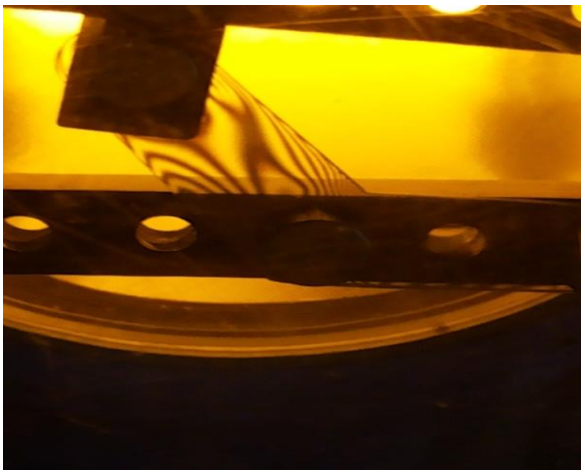

Figure 8 Bell crank lever at 135^0 in Circular polariscope

Table 8 Determination of Stresses using photoelasticity of Bell Crank Lever at 135^0

S.NO	Load(kg)	Fringe Order, N	σ = NFσ/h (MPa)
1	10.2	4.67	12.09
2	15.3	7.15	18.51
3	20.4	9.4	24.45

From above table 8, it is observed that, as the load increases, the principal stress also increases.

III.iv Bell Crank Lever at 160^0:

The bell crank lever at 160^0 is kept in the circular polariscope arrangement for determining the stresses. At different loads the stresses are found which are noted in below table.

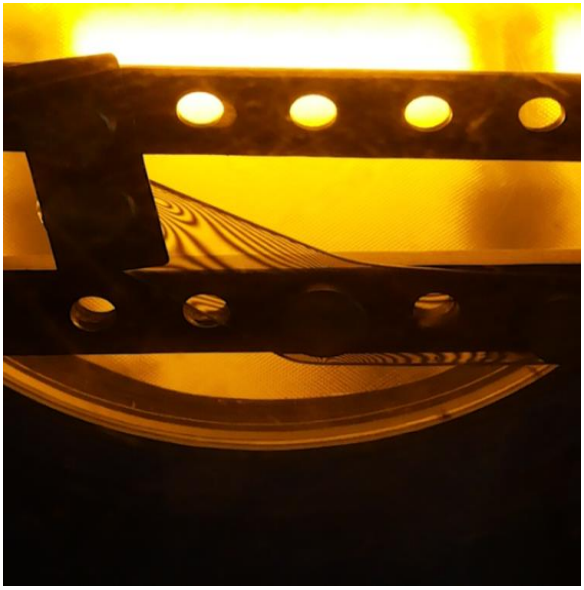

Figure 9 Bell crank lever at 160^0 in Circular polariscope

Table 9 Determination of Stresses using photoelasticity of Bell Crank Lever at 160^0

S.NO	Load(kg)	Fringe Order, N	σ = NFσ/h (MPa)
1	10.2	4.64	12.01
2	15.3	6.92	17.9
3	20.4	9.28	24.02

From the above table 9, it is observed that, as the load increases, the principal stress also increases. The results obtained experimentally using photoelastic

bench equipment by photoelastic stress analysis under whole field technique at different conditions is graphically shown in fig. 10. By comparing the results between theoretical and experimental, from the graphs shown in figures 5 and 10, it is observed that results obtained are in close agreement with each other.

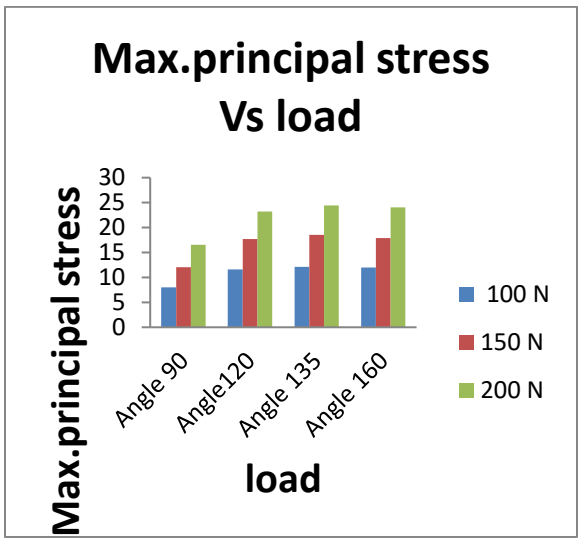

Figure 10 Effect of angle between two arms on max.principal stress (Experimental)

IV. Stress Analysis by Numerical Method (Finite Element Analysis):

By using ANSYS WORKBENCH, the stress analysis was done at four different angles of bell crank lever between load arm and effort arm at three different loads which are 100N, 150N, and 200N. In this the maximum principal stress and maximum shear stress are found by varying the load. In the bell crank lever, the load is applied at the lever section in the downward direction, the effort is applied at arm section in the horizontal direction and it is fixed at the fulcrum of the bell crank lever with fulcrum pin.

IV.i Bell Crank Lever at 90^0:

a) Maximum Principal Stress when Bell Crank Lever of 90^0 subjected to 100N, 150N and 200N Load:

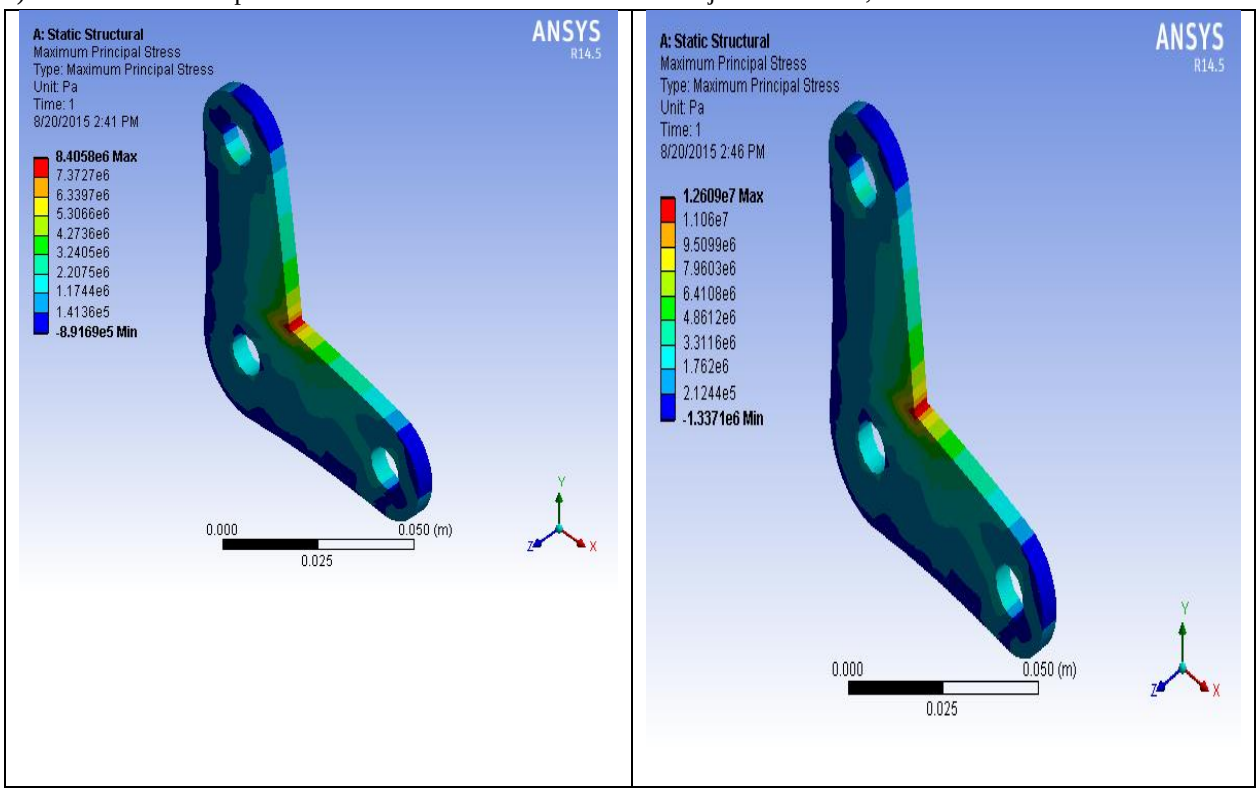

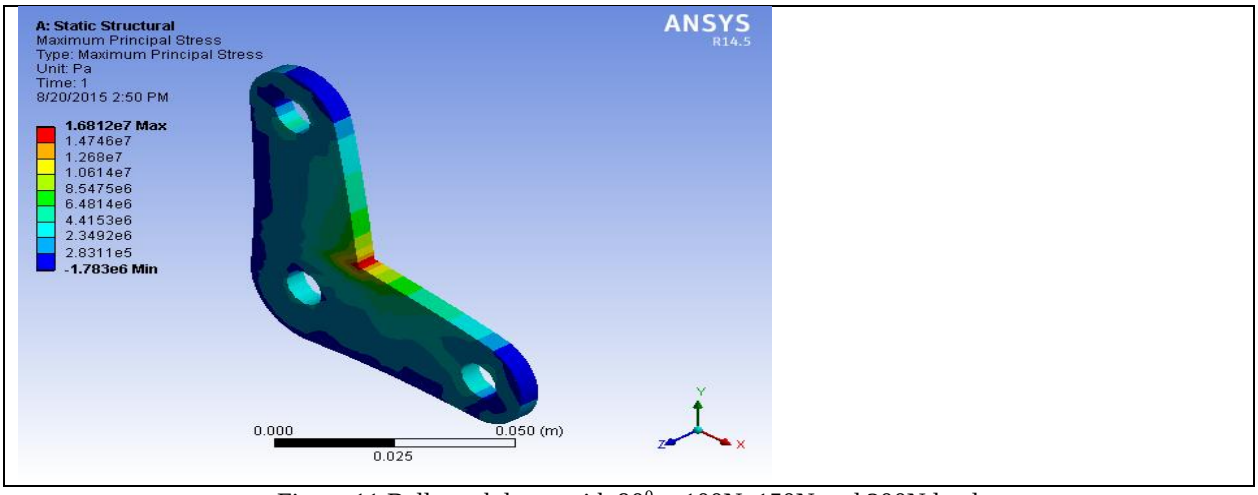

Figure 11 Bell crank lever with 90^0 at 100N, 150N and 200N load

IV.ii Bell Crank Lever at 120^0:

a) Maximum Principal Stress when Bell Crank Lever of 120^0 subjected to 100N, 150N and 200N Load:

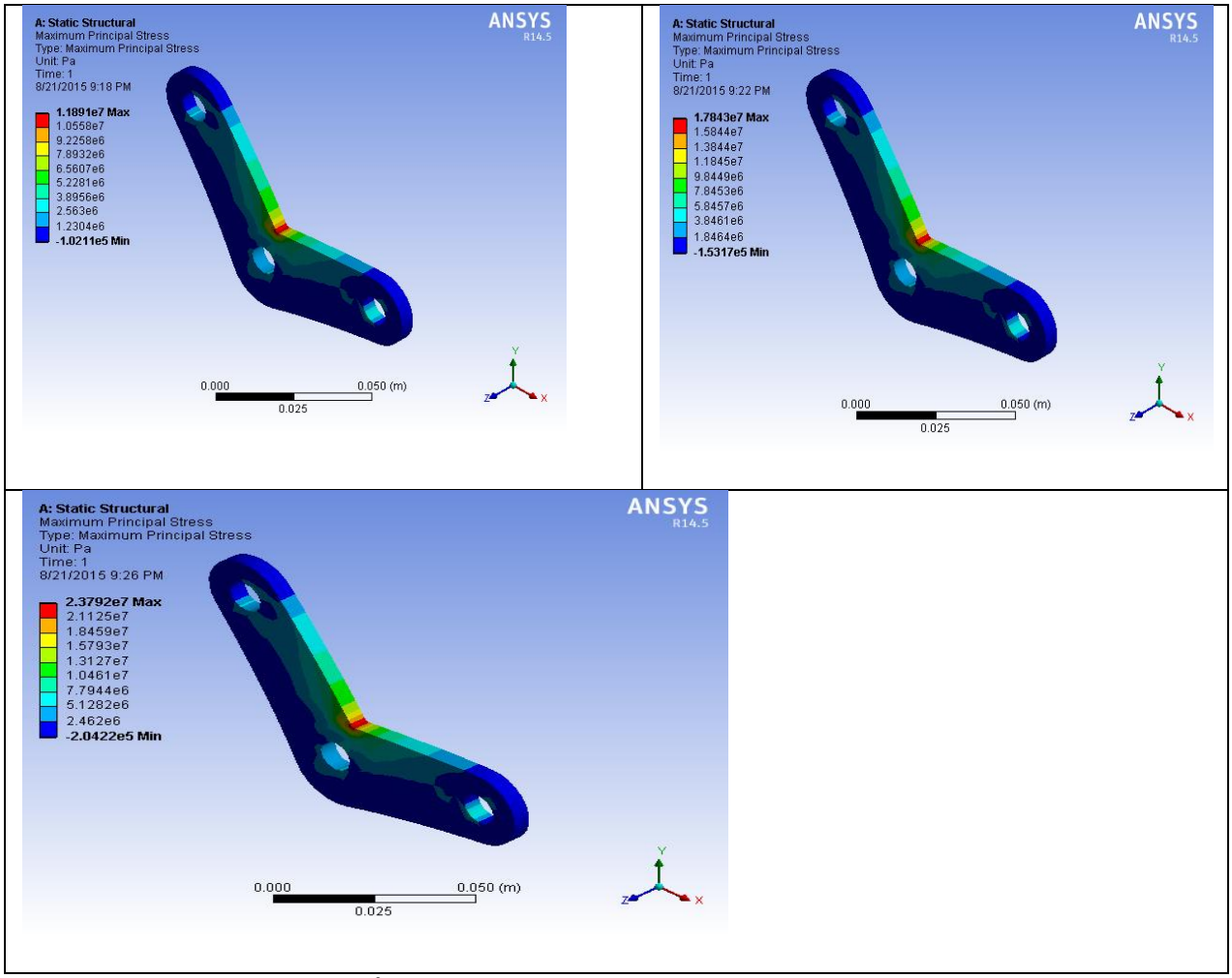

Figure 12 Bell crank lever with 120^0 at 100N, 150N and 200N load

IV.iii Bell Crank Lever at 135^0:

a) Maximum Principal Stress when Bell Crank Lever of 135^0 subjected to 100N, 150N and 200N Load:

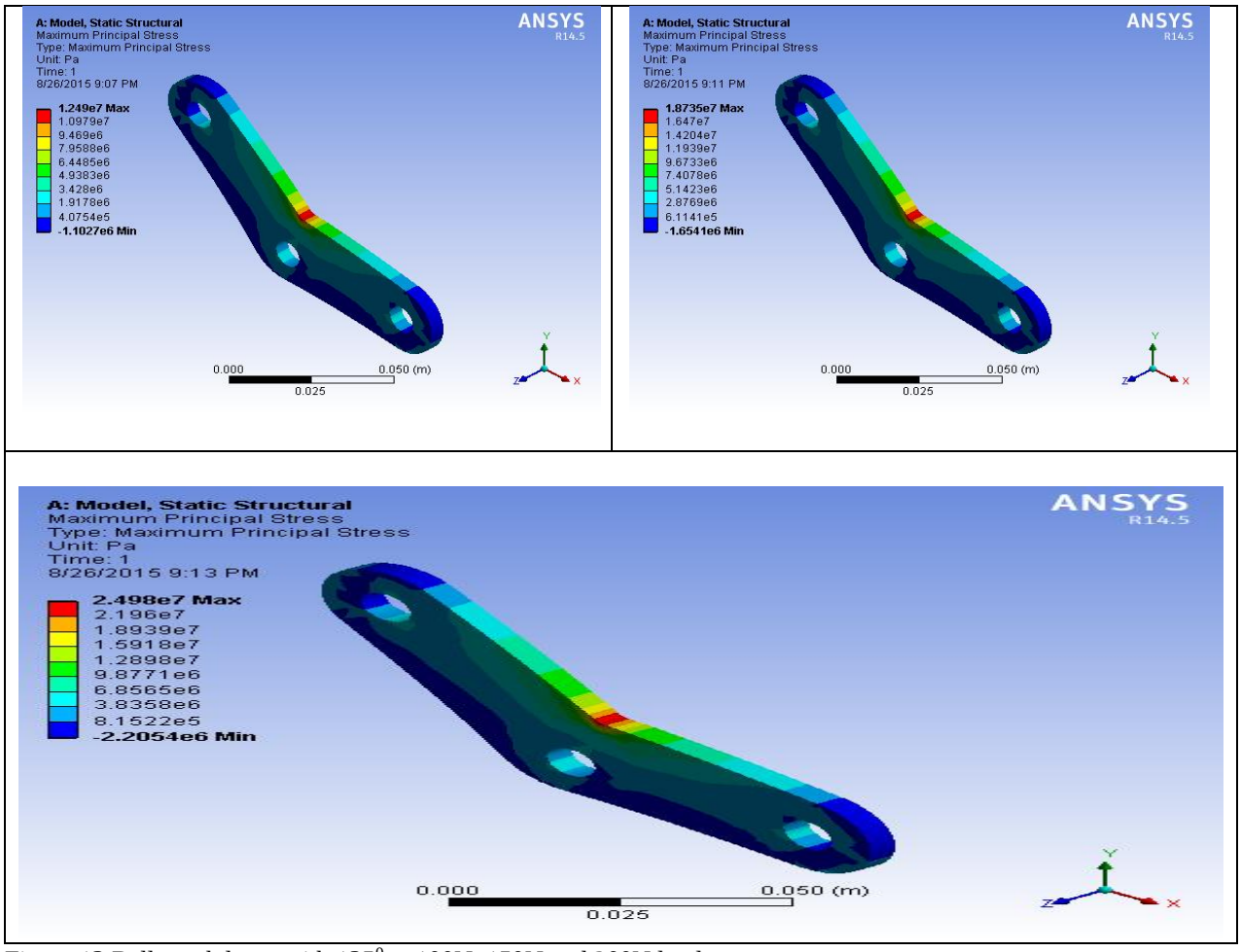

Figure 13 Bell crank lever with 135^0 at 100N, 150N and 200N load

IV.iv. Bell Crank Lever at 160^0:

a) Maximum Principal Stress when Bell Crank Lever of 160^0 subjected to 100N, 150N and 200N Load:

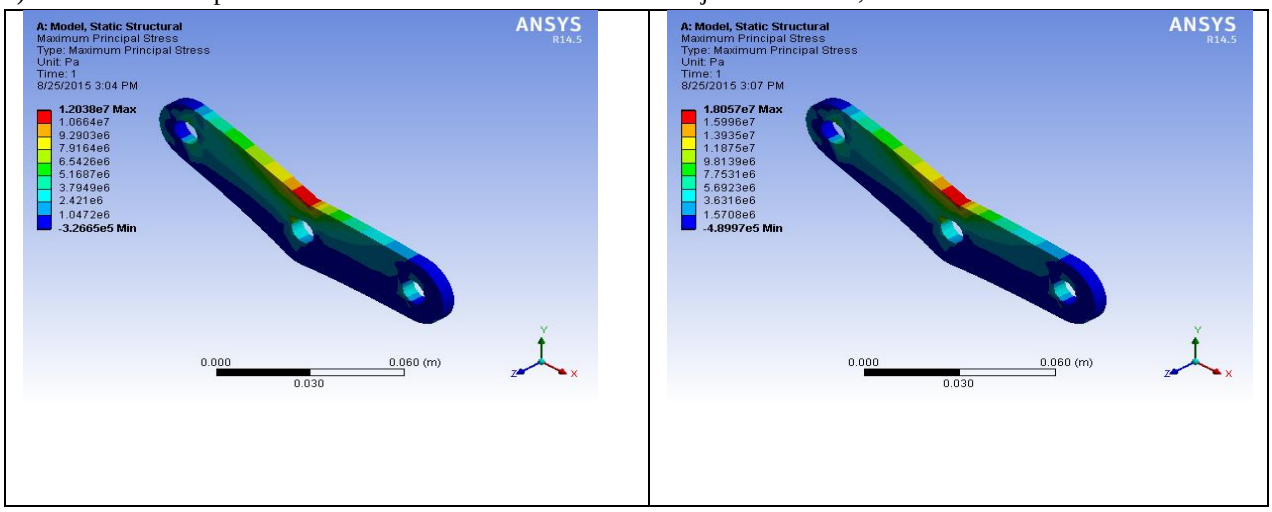

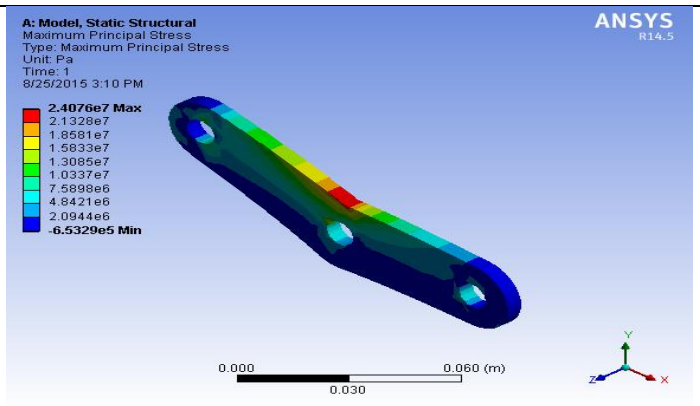

Figure 14 Bell crank lever with 160^0 at 100N, 150N and 200N load

Table 10 Analysing stresses induced in lever by using ANSYS WORKBENCH

Angle (N)	Load (N)	Effort (N)	ANSYS WORKBENCH (MPa)	
			σ_{max}	τ_{max}
90^0	100	90.90	8.40	4.09
	150	136.36	12.60	6.14
	200	181.81	16.81	8.19
120^0	100	104.9	11.89	5.79
	150	157.45	17.84	8.69
	200	209.94	23.79	11.6
135^0	100	128.55	12.49	6.2
	150	192.84	18.73	9.15
	200	257.12	24.98	12.21
160^0	100	265.8	12.03	5.98
	150	398.7	18.05	8.97
	200	531.6	24.07	11.97

From the above table 10, it is observed that, as the load increases, then effort increases and then the maximum principal stress and shear stress also increases. The results are graphically shown in fig. 4.26.

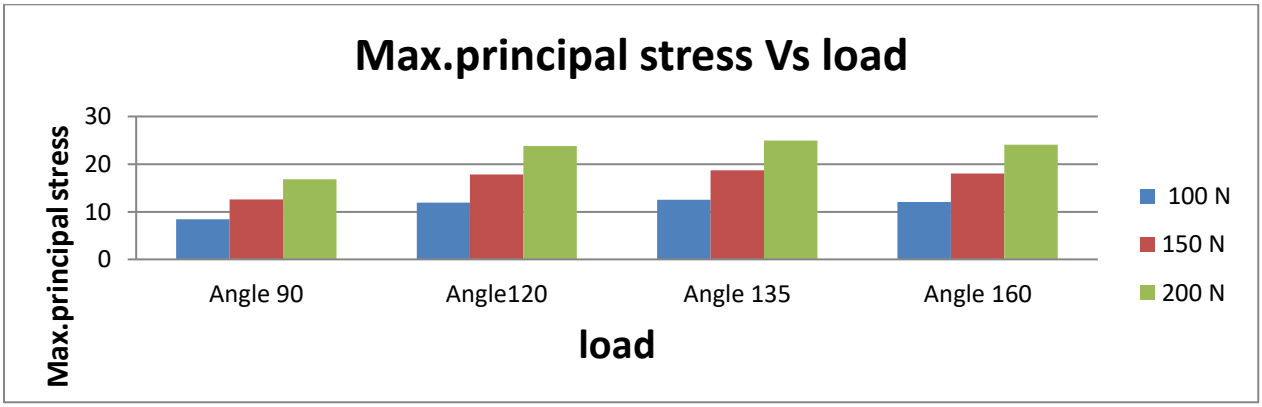

Figure 15 Effect of angle between two arms on max.principal stress (ANSYS)

V MATLAB:

In MATLAB, the stresses at the lever section and the fulcrum pin are found by different programs.

V.i The Stress at Lever Section: By using this program for lever section the maximum principal stress was found by varying the load.

```
clc
clear
b=5;
h=25;
l=50;
d=25;
for i=1
   for W=200
      iter =1;
      M=W*(l-(d/2));
      Z= (b*(h)^2)/6;
      Principal stress=M/Z;
      Shear stress=W/(b*h);
Maximum principal stress(i)=(principal stress/2)+(1/2)*(sqrt((principal stress)^2 )+(4)*(shear stress)^2);
maximum shear stress(i)=(1/2)*(sqrt((principal stress)^2)+(4)*(shear stress)^2);
iter=iter+1;
   end;
end;
```

As discussed in II.i, the remaining stresses also calculated by using above standard programs by varying load and resultant forces.

Table 11. stresses at different angles and at different loads by using MATLAB program at lever section.

Angle	Load (N)	MATLAB at Lever (Mpa)	
		σ_{max}	τ_{max}
90^0	100	8.48	4.88
	150	13.68	8.28
	200	19.52	12.32

From the above table 4.12, it is observed that, stress values increase with the load.

V.ii The Stress at the Fulcrum pin**:** By this program the maximum principal stress was found by resultant force (R_F).

```
clc
clear
t=5;
l=35;
d=10.18;
for i=1
   for R=135.14
      iter=1;
      M=(R/2)*(l/4 + t/3);
      Z=(Π/32)*d^3;
     Principal stress=M/Z;
    Shear stress=(2*R)/(Π*d^2);
 Maximum principal stress(i)= (principal stress/2)+(1/2)*(sqrt((principal stress)^2)+(4)*(shear stress)^2);
 Maximum shear stress(i)=(1/2)*(sqrt((principal stress)^2)+(4)*(shear stress)^2);
      iter=iter+1;
   end;
end;
```

As discussed in II.i, the remaining stresses also calculated by using above standard programs by varying load and resultant forces.

Table 12 stresses at different angles and at different loads by using MATLAB programs at the fulcrum pin section.

Angle	Load (N)	Resultant force (N)	MATLAB at Fulcrum pin (Mpa)	
			σ_{max}	τ_{max}
90^0	100	135.14	6.89	3.49
	150	202.72	10.34	5.24
	200	270.30	13.78	6.99
120^0	100	177.46	9.05	4.59
	150	266.30	13.58	6.88
	200	355.05	18.10	9.18
135^0	100	211.43	10.78	5.47
	150	317.16	16.17	8.20
	200	422.90	21.57	10.94
160^0	100	361.40	18.43	9.35
	150	542.08	27.64	14.02
	200	722.80	36.86	18.70

From the above table 12, it is observed that, stress values increase with the load.

V.iii. Comparison of Results:

The Bell Crank Lever was analyzed by the methods which are Theoretical method, Experimental method (Photoelasticity), Numerical method (Finite Element Analysis), MATLAB.

Table 13 Comparison of results

Angle	Load (N)	Effort (N)	Theoretical at Fulcrum pin (Mpa)		Photoelas--ticity (Mpa)		ANSYS WORKBENCH at Lever section (Mpa)		MATLAB at Fulcrum pin(Mpa)	
			σ_{max}	τ_{max}	σ_{max}	τ_{max}	σ_{max}	τ_{max}	σ_{max}	τ_{max}
90^0	100	90.90	6.89	3.49	8.01	4.03	8.40	4.09	6.89	3.49
	150	136.36	10.34	5.24	12.03	6.01	12.60	6.14	10.34	5.24
	200	181.81	13.79	6.99	16.52	8.27	16.81	8.19	13.78	6.99
120^0	100	104.9	9.05	4.59	11.58	5.64	11.89	5.79	9.05	4.59
	150	157.45	13.58	6.89	17.72	8.67	17.84	8.69	13.58	6.88
	200	209.94	18.11	9.18	23.19	12.57	23.79	11.6	18.10	9.18
135^0	100	128.55	10.78	5.47	12.09	6.04	12.49	6.2	10.78	5.47
	150	192.84	16.18	8.21	18.51	9.14	18.73	9.15	16.17	8.20
	200	257.12	21.57	10.94	24.45	12.25	24.98	12.21	21.57	10.94
160^0	100	265.8	18.43	9.35	12.01	6.02	12.03	5.98	18.43	9.35
	150	398.7	27.66	14.03	17.9	8.73	18.05	8.97	27.64	14.02
	200	531.6	36.87	18.70	24.02	12.15	24.07	11.97	36.86	18.70

From the above table 13 as the load increases, the effort increases and maximum principal stress and maximum shear stress also increases. The optimum angle is 90^0.

VI. CONCLUSION:

From the above results the Bell Crank Lever was analyzed by the methods which are Theoretical, Experimental (Photoelasticity), Numerical method (Finite Element Analysis), MATLAB and the following conclusions were obtained:

1. As the load increases at different angles of Bell Crank Lever, the Effort and also Resultant Force increases. The minimum effort that can be applied for a load is observed at an angle of Bell Crank Lever is 90^0.
2. As the angle between the lever arms increases, the Mechanical Advantage decreases.
3. At lever section and fulcrum pin, as the load and angle between the arms increases, the maximum principal and shear stresses also increases. And the optimum angle is observed at 90^0.
4. By comparing the results obtained by theoretical, experimental, analytical and from MATLAB, reveals that they are in close agreement with each other.

REFERENCES

[1] Prof. Vivek C. Pathade, DR. Dilip S. Ingole, “Stress Analysis of I.C.Engine Connecting Rod by FEM and Photoelasticity” IOSR Journal of Mechanical and Civil Engineering (IOSR-JMCE) e-ISSN: 2278-1684 Volume 6, Issue 1 (Mar. - Apr. 2013), PP 117-125.

[2] Bhosale Kailash C. “Photoelastic Analysis of Bending Strength of Helical Gear” Innovative Systems Design and Engineering.

[3] Shetty Prajna P, Patil N Konark, Meshramkar Roseline, Nadiger Ramesh K. “A Fast and Economical Photoelastic Model Making of the

Teeth and Surrounding Structure" Issue 5 (Jan.-Feb. 2013).
[4] Fred M. Discenzo, Charles E. Mitchell, Dukki Chung, Donald D. Theroux. **"**Photo-elastic sensor provides unique torque information for diagnostics and control"
[5] Tae Hyun Baek, Myung Soo Kim, Dong Pyo Hong. "Fringe Analysis for Photoelasticity Using Image Processing Techniques".
[6] Mr. M. M. Dange, Prof. S. R. Zaveri, Prof.S.D.Khamankar. "Stress Analysis of Bell Crank Lever"
[7] Rao Venkateswara P, Rao Kannaji A, Rao Kameswara T.V. Araldites for Photo- Elastic Studies and Their Transition Temperatures Jpn. J. Appl. Phys.
[8] Badran Serene A., Orr John F., Stevenson Mike and Burden Donald J. Photo-elastic stress analysis of initial alignment arch wires.
[9] Dally, J. W., and W. F. Riley. 1991. Experimental Stress Analysis, 3rd ed. New York: McGraw-Hill.
[10] Tada, P.C. Paris, and G. R. Irwin. 1985. Stress Analysis of Cracks Handbook, 2nd ed. St. Louis, Mo.: Paris Productions, Inc.
[11] Pai, C. L., 1996, "The shape optimization of a connecting rod with fatigue life constraint," Int. J. of Materials and Product Technology.
[12] Pravardhan S. Shenoy, "Dynamic load analysis and optimization of connecting rod", 2004, Master's thesis, University of Toledo.
[13] Ashokan K, and Ramesh, K., 2009, "Finite element simulation of isoclinic and isochromatic phasemaps for use in digital photoelasticity", Experimental Techniques.
[14] Baek, T.H., Kim, M.S., Morimoto, Y. and Fujigaki, M., 2002, "Separation of isochromatics and isoclinics from photoelastic fringes in a circular disk by phase measuring technique".
[15] Corso, F.D., Bigoni, D. and Gei, M., 2008, "The stress concentration near a rigid line inclusion in a pre-stressed, elastic material. Part I: Full-field solution and asymptotics".
[16] H.T.Jessop, and F. C. Harris, Photoelasticity Principles and Methods (Mineola, N.Y.Dover Publications, Inc., 1952).
[17] Doyle, F. (2004). Modern Experimental Stress Analysis: Completing the solution of partially specified problems. Chichester: John Wiley & Sons Ltd.
[18] Ramachandra, K., et al., Stress Analysis and optimisation of turbine rotor blade shrouds, Proceeding Eighth International Symposium on Air Breating Engines, Cincinatti, USA, 1987, pp. 3-5.
[19] M.M.Frocht, Photoelasticity (New York: John Wiley and Sons, **1**, 382 1941).
[20] D.Vassarheli, Contribution to the calculation of stresses from photoelastic values, Proc. SESA, **9**(1) (1951).
[21] Assif D, Oren E, Marshak BL, Aviv I. Photoelastic analysis of stress transfer by endodontically treated teeth to the supporting structure using different restorative techniques. J Prosthet Dent 1989;61: 535-43.
[22] Muhammad sahail bin zainol abiding-universiti teknikal, "Design and Development of a Bell Crank for mono shock front suspension for fomula varsity race car". Malaysia May-2011
[23] Robert L. Johnson, "Model Making and Slicing for Three-Dimensional Photoelasticity", Experimental Mechanics, March 1969, pp 23-32
[24] Gary Alan Manney, A thesis on "Investigation of Epoxy Resins for use in Photoelasticity", Texas Technology College, May 1965.
[25] N.V.Scurria and J.F.Doyle, "Photoelastic Analysis of Contact Stresses in the presence of Machining Irregularities", September 1982, pp. 342-347.
[26] Thomas L. Dolan, "A Photoelastic Study of Stresses in Gear Tooth Fillets",University of Illinois Engineering Experiment Station, Bulletin No 335.
[27] S.Timoshenko and J.N.Goodier, "Theory of Elasticity", McGrawhill Book Company, pp 131-143.
[28] James W.Dally, William F.Riley, "Experimental Stress Analysis", McGrawhill Book Company, pp 374.
[29] Dr.Sadhu Singh, "Experimental Stress Analysis",Khanna Publications, Fourth Edition 2009, pp 281-392.
[30] V.B.Bhandagi – Design of Machine Elements, Tata Mcgraw-Hill.